IEEE Access
Multidisciplinary | Rapid Review | Open Access Journal

Received March 13, 2019, accepted March 21, 2019, date of current version May 6, 2019.

Digital Object Identifier 10.1109/ACCESS.2019.2907674

State Constrained Variable Structure Control for Active Heave Compensators

HUAN YU[1], YING CHEN[2], WENZHUO SHI[1], YI XIONG[3], AND JIANHUA WEI[1]
[1]State Key Laboratory of Fluid Power and Mechatronic Systems, Zhejiang University, Hangzhou 310027, China
[2]Hangzhou Applied Acoustics Research Institute, Hangzhou 310023, China
[3]Nantong Metalforming Equipment Co., LTD, Nantong 226578, China

Corresponding author: Wenzhuo Shi (wzshi09@163.com)

ABSTRACT Heave compensation systems are widely used to decouple the load motion from wave-induced vessel motion for the equipment handling on the ocean. Researches have been made to achieve successful compensation, yet few of them discusses the inherent constraints of the systems, such as bounded compensator's stroke and max actuator's velocity. This paper presents a solution for active heave compensation systems with such constraints by means of variable structure control. The controller's complexity on design procedures and effectiveness are compared with a trajectory planning control method which turns out that the variable structure controller is more suitable to apply to the active heave compensators. The back-stepping method is used to robustly stabilize this variable structure system and for the aim of a decrease on the high robust gain due to uncertain friction term, a modified decoupled friction observer is used which is also verified by both theoretical and experimental analyses. To compensate for the time delay of the motion reference unit (MRU), a heave prediction algorithm is used. The experimental results show that most heave motion can be compensated when the motion and its velocity are feasible, while no hit occurs otherwise.

INDEX TERMS Heave compensation, nonlinear state constrained control, variable structure system, heave prediction, nonlinear friction observer.

I. INTRODUCTION

Vessel heave motion resulting from the sea swell and wind waves can significantly affect the offshore operations such as drilling, deep sea mining, payload transfer, dredging, hydrographic surveying, etc. [1]–[4]. Heave compensation systems are used to compensate such movement as much as possible and the past 40 years have seen heave compensation systems to become commonplace in many maritime operations [5].

There are mainly three categories of compensation systems: passive heave compensation system (PHC), active heave compensation system (AHC) and hybrid active-passive heave compensation system (HAHC). PHCs are mechanical vibration isolators composed of hydraulic cylinders and accumulators which require no input energy to function whereas the heave motion reduction is no more than 80% after many researches on dynamic behaviors, mechanical structures and parameter influences [6]–[9]. An effective way to improve the compensator's performance is to add active parts into the compensation system resulting in AHCs or HAHCs. AHCs based on hydraulic winch or hydraulic cylinders can both get good compensating results using proper heave prediction algorithm and robust nonlinear controllers [9], [10]. In comparison with winch based AHCs, cylinder based ones have two obvious advantages. One is that the inertia of a hydraulic cylinder is usually smaller than a winch thus systems based on cylinders are easier to get a better control performance. The other is that cylinders are easier to be combined with accumulators which can directly decrease the totally installed power of the system. Meanwhile, a shortcoming of cylinder based AHC is the limitation on cylinder's stroke which can do serious damage to the equipment and the staff when sea condition is high and this is the problem aimed to be handled in this paper.

During the process of successful compensation, if the vessel's heave motion induced by a sudden big wave exceeds the predesigned stroke of the compensator's cylinder and the motion is compensated by the previous control law, velocity of the compensation system will not be zero on the stoppage of its mechanical structure which then leads to a collision and serious accident will happen in turn. This problem is also raised in [5], [10] and the current solution is to lock

The associate editor coordinating the review of this manuscript and approving it for publication was Wenchao Meng.

the compensator entirely to avoid hits [9], [11]. Obviously adaptability of such solution is poor and performance of such compensators is quite limited since a sufficient stroke of the cylinder need to be reserved in case of hits. Besides stroke limitation, service life of the compensator may be decreased in the same way resulting from occasional over speed.

From the control point of view there are two methods that can be used to solve the problem. One is to refine the target compensated trajectory first so that the practical compensated heave is within the system's compensating range, or feasible area, of the controllers' require, then use the state constrained controller derivation methods to guarantee the boundedness of velocity and acceleration during the working process. Methods can be used to derive such controllers including model predictive control [12], [13], reference governors [14], the use of set invariance control [15]–[17] and barrier Lyapunov function [18]–[21]. The other solution to constrain tracking trajectory is to use variable structure control, that is, when the trajectory is within the feasible area, tracking controller is used; when it exceeds the position, velocity or acceleration range, corresponding boundary controller is used so that the states can slide on the boundary until tracking is feasible to be fulfilled again. Note that boundary controller requires high robustness and the regulation space should be as small as possible such that the cylinder's stroke can be fully used to compensate the heave motion. With this consideration in mind regulation process to the boundary is designed as a near time optimal response with the max allowable acceleration [22], [23].

Besides the variable structure control law, a heave prediction algorithm is suggested to overcome the delays in the system [24] and the benefit is verified in [9], [10]. In this paper a sliding mode observer based prediction algorithm is used [25]. To finish the controller design, disturbance and uncertainties in the system need to be considered. Many advanced closed-loop controllers are proposed to improve the performance of the intrinsically nonlinear and uncertain hydraulic systems [26]–[28], [30]. In this paper a backstepping method is employed to handle the unmodeled disturbances, meanwhile friction is observed by a decoupled nonlinear friction observer originally proposed in [31] and modified in this paper. This observer can decrease the robust gain and make it easier to tune parameters of the controller which in turn makes the controller more suitable for industrial applications, moreover, the observed friction can be used to the offline simulation model of the system for other research interests.

Structure of this paper is organized as follows. In section 2 preliminary components are introduced including system's working principle and its dynamic model, heave prediction algorithm and the modified nonlinear friction observer. A comparison in state constrained control between the two solutions mentioned above is given in section 3. In section 4 a robustly state constrained variable structure control algorithm is proposed. Effectiveness of the control algorithm is verified by experimental results in section 5.

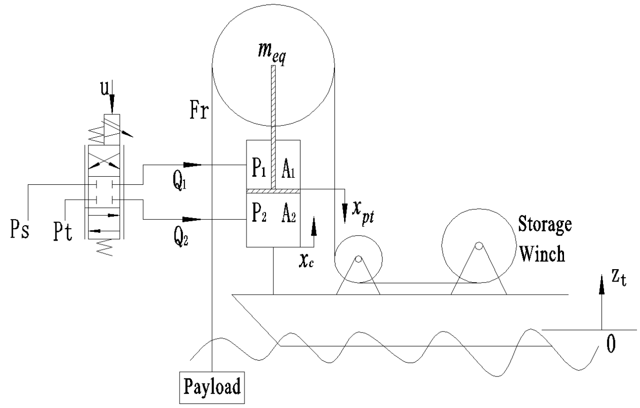

FIGURE 1. Schematic of the AHC system.

At the end of this paper conclusions are given and some further research points are put forward.

II. PRELIMINARY COMPONENTS

A. WORKING PRINCIPLE AND DYNAMIC MODEL

Schematic of this AHC is shown in Fig.1. A movable pulley is braced by rod of a plunger cylinder whose chambers are controlled by a servo valve. The piston area, pressure and volume of the rodless chamber together with the flow rate into this chamber are defined as A_2, P_2, V_2, Q_2 respectively and those of the rod chamber are defined as A_1, P_1, V_1, Q_1. A cable is around the movable pulley with the payload on one end and a storage winch on the other. The storage winch is used to lift or release the payload and here it is assumed to be static. Movement of the piston is marked as x_{pt} and its coordinate is fixed on the cylinder with the origin in the middle of the cylinder, and z_t is the vessel's heave relative to zero sea level in vertical direction. Positive directions of these movements are shown in the figure.

Take the state variables as $x_1 = x_{pt}, x_2 = \dot{x}_{pt}, x_3 = P_1, x_4 = P_2$, state equations of the system can be written as follows

$$\begin{aligned}
\dot{x}_1 &= x_2 \\
\dot{x}_2 &= \frac{1}{m_{eq}}\left(f_2 - \hat{F}_f - \delta F_f + A_1\bar{x}_3\right) \\
\dot{\bar{x}}_3 &= f_4 u - f_3 - f_5
\end{aligned} \tag{1}$$

where F_r is the tension of the cable, m_{eq} is the equivalent mass of the cable, movable pulley and the payload; g is the gravitational constant; F_f is the mechanical friction written as $F_f = \hat{F}_f + \delta F_f$, with $\hat{F}_f$ being the estimate from the nonlinear friction observer aforementioned and δF_f being a small residual.

Other functions and parameters are defined as below

$$\begin{aligned}
\alpha &= \frac{A_2}{A_1} \\
\bar{x}_3 &= x_3 - \alpha x_4 \\
f_2 &= 2F_r + m_{eq} g
\end{aligned}$$

$$\begin{aligned} f_3 &= \left(h_1 A_1 \dot{x}_{pt} + h_2 A_2 \dot{x}_{pt}\right) \\ f_4 &= h_1 g_1 + h_2 g_2 \\ f_5 &= h_1 C_t \left(x_3 - x_4\right) - h_2 C_t (x_4 - x_3) \end{aligned} \tag{2}$$

with

$$\begin{aligned} g_1 &= k_q \sqrt{P_s - P_1} sign\left(u\right) + k_q \sqrt{P_1 - P_t} sign\left(-u\right) \\ g_2 &= k_q \sqrt{P_2 - P_t} sign\left(u\right) + k_q \sqrt{P_s - P_2} sign(-u) \\ h_1 &= \frac{\beta_e}{V_{01} + A_1 x_{pt}} \\ h_2 &= \frac{\beta_e}{V_{02} - A_2 x_{pt}} \end{aligned} \tag{3}$$

where β_e is the hydraulic fluid bulk modulus, V_{01}, V_{02} are initial values of V_1, V_2; C_t is the leakage coefficient of cylinder.

B. HEAVE PREDICTION ALGORITHM

A heave prediction algorithm for AHC to improve the compensation performance is proposed in [9] based on kalman observer (KOPA) and the benefit is verified in [9], [10], but one important part of KOPA is not described in detail known as peak detection algorithm (PDA). It has been pointed out that without a proper PDA, it is not easy to get the prediction results as good as the one in [9]. Hence a sliding mode observer based prediction algorithm (SMOPA) is designed in [25] which has been proved to be effective according to the measured data of sea trials.

Wave induced vessel motion $w\left(t\right)$ can be decomposed into a set of sine waves which are called modes, as proposed in [32], [33]

$$w\left(t\right) = \sum_{i=1}^{N} A_i sin(2\pi f_i t + \varphi_i) + q\left(t\right) \tag{4}$$

where A_i, f_i, φ_i are the amplitude, frequency and phase of mode i. It has been verified by numerical simulation that a good prediction can be made without the unknown term $q(t)$, so only N modes are considered in the design of SMOPA. The ordinary differential equation of mode i can be described as follows

$$\begin{aligned} \dot{x}_i &= \begin{bmatrix} 0 & 1 \\ -\left(2\pi f_i \left(t_0\right)\right)^2 & 0 \end{bmatrix} \boldsymbol{x_i} = \boldsymbol{A_i x_i} \\ w_i\left(t\right) &= \begin{bmatrix} 1 & 0 \end{bmatrix} \boldsymbol{x_i} = \boldsymbol{C_i x_i} \\ i &= 1, 2, 3 \ldots N \end{aligned} \tag{5}$$

It is obvious that mode i is observable and a combination of these modes in (3) is also observable, yields the observability of system:

$$\begin{aligned} \dot{\boldsymbol{x}}(t) &= \begin{bmatrix} \boldsymbol{A_1} & 0 & \ldots & 0 \\ 0 & \boldsymbol{A_2} & \ldots & 0 \\ \vdots & \vdots & \ddots & \vdots \\ 0 & 0 & \cdots & \boldsymbol{A_N} \end{bmatrix} \boldsymbol{x} = \boldsymbol{Ax} \\ w\left(t\right) &= \begin{bmatrix} \boldsymbol{C_1} & \boldsymbol{C_2} & \ldots & \boldsymbol{C_N} \end{bmatrix} \boldsymbol{x} = \boldsymbol{Cx} \end{aligned} \tag{6}$$

Utkin [34] proposes a sliding mode observer for the system mentioned above:

$$\begin{aligned} \dot{\hat{\bar{\boldsymbol{x}}}} &= \bar{\boldsymbol{A}} \hat{\bar{\boldsymbol{x}}} + \bar{\boldsymbol{G}}_{\mathbf{n}} v \\ \hat{w} &= \bar{\boldsymbol{C}} \hat{\bar{\boldsymbol{x}}} \end{aligned} \tag{7}$$

where

$$\begin{aligned} \bar{\boldsymbol{A}} &= \boldsymbol{T_c A T_c^{-1}} = \begin{bmatrix} \boldsymbol{A_{11}} & \boldsymbol{A_{12}} \\ \boldsymbol{A_{21}} & \boldsymbol{A_{22}} \end{bmatrix} \\ \bar{\boldsymbol{C}} &= \boldsymbol{C T_c^{-1}} = [0 \;\; 0 \ldots 0 \;\; 1] \end{aligned}$$

$$\begin{aligned} &\boldsymbol{A_{11}} \in \boldsymbol{R}^{(2N-1)\times(2N-1)}, \quad \boldsymbol{A_{21}} \in \boldsymbol{R}^{1\times(2N-1)}, \\ &\boldsymbol{A_{12}} \in \boldsymbol{R}^{(2N-1)\times 1}, \quad \boldsymbol{A_{22}} \in \boldsymbol{R}^{1\times 1} \end{aligned}$$

$\boldsymbol{T_c}$ is a diffeomorphism coordinate translation $\bar{\boldsymbol{x}} = \boldsymbol{T_c x}$ that can transform the system into the observable canonical form due to the observability of system and $\hat{\bar{x}}$ is the estimate of $\bar{\boldsymbol{x}}$; $\bar{G}_{\boldsymbol{n}} = \begin{bmatrix} \boldsymbol{L} \\ -1 \end{bmatrix}, \boldsymbol{L} \in \boldsymbol{R}^{(2N-1)\times 1}$. With a proper choice of $\boldsymbol{L}$ [35], estimation error will converge to zero in finite time. Then according to the mode parameter extraction procedure in [9] from the observed states, predicted heave motion $w(t)$ together with its velocity $\dot{w}(t)$ and acceleration $\ddot{w}(t)$ can be calculated.

C. NONLINEAR FRICTION OBSERVER

Nonlinear friction is extensively described by LuGre model [35]:

$$F_f = \sigma_0 z + \sigma_1 \dot{z} + \sigma_2 v \tag{8}$$

where σ_0, σ_1 and σ_2 are friction force parameters, which can be physically interpreted as the stiffness of the bristles between two contact surfaces, damping coefficient of the bristles and viscous coefficient, respectively; v is the velocity; the unmeasurable internal friction state is governed by

$$\dot{z} = v\left(1 - \frac{1}{g\left(v\right)} z\right) \tag{9}$$

where

$$g\left(v\right) = \left(f_c + \left(f_s - f_c\right) e^{-\left(\frac{v}{v_s}\right)^2}\right) sign\left(v\right) = f(v) sign(v)$$

$$sign\left(*\right) = \begin{cases} 1 & * > 0 \\ 0 & * = 0 \\ -1 & * < 0 \end{cases}$$

with f_c, f_s, v_s being coulomb friction, static friction and stribeck velocity, the following transformation can be performed

$$\begin{aligned} F_f &= \sigma_0 z + \sigma_1 v \left(1 - \frac{1}{f\left(v\right)} sign\left(v\right) z\right) + \sigma_2 v \\ &= sign\left(v\right) \left(\sigma_0 z sign\left(v\right) + \left(\sigma_1 + \sigma_2\right) \left|v\right| - \frac{\sigma_1 v}{f\left(v\right)} z\right) \\ &= a\left(t, v\right) sign\left(v\right) \end{aligned} \tag{10}$$

In [31] a nonlinear friction observer for friction described by (10) is put forward. To make control signal smoother, a modified structure for friction is preferred as:

$$F_f = a * tanh(v/eps) \tag{11}$$

where *eps* is a small positive constant. It is to be proved that the observer in [31] will also converge to F_f in the structure of (8).

Dynamic system and the form of nonlinear observer are as follows

$$\begin{aligned} \dot{v} &= -F_f(v, a) + w_F \\ \hat{a} &= z_f - k|v|^{\mu} \end{aligned} \tag{12}$$

where w_F stands for the total force and dynamic of z_f is

$$\dot{z}_f = k\mu |v|^{\mu-1}\left(w_F - F_f\left(v, \hat{a}\right)\right) sign(v) \tag{13}$$

Define the error of a as

$$e = a - \hat{a}$$

Then the error dynamic is given by

$$\begin{aligned} \dot{e} &= -\dot{\hat{a}} = -\dot{z}_f + k\mu|v|^{\mu-1}\dot{v}sign(v) \\ &= k\mu|v|^{\mu-1} sign(v) \\ &\quad \times \left(\hat{a} * tanh\left(\frac{v}{eps}\right) - a * tanh\left(\frac{v}{eps}\right)\right) \\ &= -ek\mu|v|^{\mu-1} sign(v) \tanh\left(\frac{v}{eps}\right) \end{aligned} \tag{14}$$

which means that for $k > 0, \mu > 0$, observer error e converges asymptotically to zero if v is bounded away from zero.

Though in this proof a is assumed to be a constant, a time varying a can still be observed by the later experimental results in this paper.

III. COMPARISON OF CONSTRAINED CONTROLLERS

In this section we will use a double integer to compare controller based on trajectory refinement with variable structure based control and give some comments in view of application to active heave compensation system.

Problem Statement:

Consider a dynamic system of the following form

$$\begin{aligned} \dot{x}_1 &= x_2 \\ \dot{x}_2 &= u \end{aligned} \tag{15}$$

where $(x_1, x_2) \in R^2$, $u \in R$ is the control; target trajectory is given by

$$x_d = \sin(2\pi(t+0.25))$$

with no loss of generality, set $t \in [0, 0.5]$.

Design a proper controller so that tracking can be fulfilled as much as possible with no constraints violation. Constraints are as follows

$$\begin{aligned} x_1 &\geq x_{1Lb} = -0.95 \\ x_2 &\geq v_{Lb} = -6 \\ u &\leq 38 \end{aligned} \tag{16}$$

A. STATE CONSTRAINED CONTROLLER

In this method the trajectory should be refined into the feasible area first thus proper state constrained controller can be derived.

To refine the target trajectory is to solve a constrained minimization problem defined as follows

$$min \int_{t_1}^{t_2} \left(\hat{x}_d(t) - x_d(t)\right)^2 dt \tag{17}$$

with the constraints defined as below

$$\begin{aligned} \hat{x}_d(t) &\geq -0.95 \\ \dot{\hat{x}}_d(t) &\geq -6 \\ \ddot{\hat{x}}_d(t) &\leq 38 \end{aligned} \tag{18}$$

where $\hat{x}_d$ is the target refined trajectory. To cope with the constraint on the second derivative, we approximate $\hat{x}_d$ with a linear combination of a basis function defined as

$$P(t) = (p_1(t), p_2(t), \ldots, p_m(t))^T \tag{19}$$

Thus derivatives of $P(t)$ is known. Trajectory $\hat{x}_d(t)$ then can be expressed as

$$\hat{x}_d(t) = \sum_{j=1}^{m} \alpha_j P_j(t) \tag{20}$$

where $\boldsymbol{\alpha}$ is the coefficients to be determined. In this way, constraints on the second derivative of $\hat{x}_d$ are converted into the algebraic constraints on $\boldsymbol{\alpha}$ written as

$$\begin{aligned} \hat{x}_d^{(i)}(t) &= \sum_{j=1}^{m} \alpha_j P_j^{(i)}(t) \\ i &= 0, 1, 2..n \end{aligned} \tag{21}$$

Here $P(t)$ is chosen to be an m-dimensional polynomial basis functions and this minimization problem can be solved. Then state constrained controller can be derived using the aforementioned techniques, for example, barrier lyapunov method [19] which will not be introduced here in detail.

B. VARIABLE STRUCTURE CONTROLLER

Variable structure controller is composed with a tracking controller and a series of states constrained controllers. According to the variable structure law, if continuing tracking will potentially break the state constraints, constrained controllers will be enabled, otherwise tracking controller is used and tracking process tends to be fulfilled. Control scheme is shown in Fig. 2 and to demonstrate the VS law in more detail, phase portraits of target trajectory and the designed constraints are shown in Fig. 3 by line $\Gamma_1(C_1C_2Q_3)$ and $\Gamma_2(C_1BAQ_1)$.

To make full use of the available value for tracking purpose, regulation distance to the lower boundary $|x_B - x_{1Lb}|$ should be as small as possible. The optimal approaching line to the lower boundary is the one with the max deceleration. However, maximum bandwidth of the closed-loop system can cause discontinuity near the lower bound at which the optimal

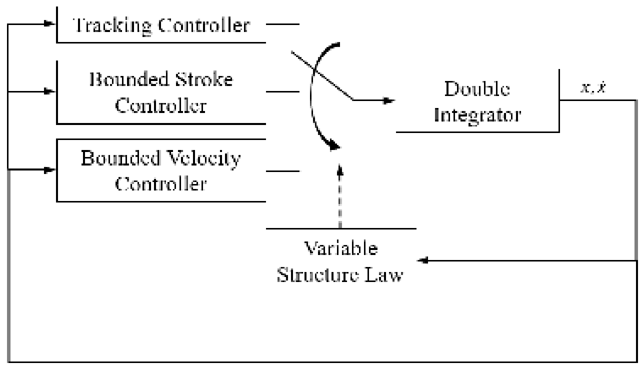

FIGURE 2. Controller scheme for the double integer.

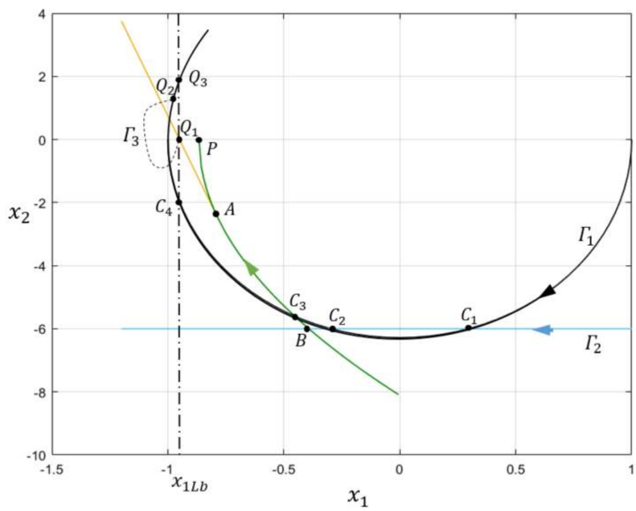

FIGURE 3. Target and constrained trajectories in phase plane.

approaching line has infinite slope [36]. To cope with this discontinuity, the approaching line is designed as a combination of a finite slope linear regulation process AQ_1 and a deceleration process BA with max admissible acceleration.

State $A(x_A, y_A)$ on BA can be described by

$$x_A = \frac{y_A^2}{2a_{Ub}} + x_P$$
$$y_A = -\sqrt{2a_{Ub}(x_A - x_P)} \tag{22}$$

State $A(x_A, y_A)$ on AQ_1 can be described by

$$y_A = -k_{OA}(x_A - x_{1L}) \tag{23}$$

with $k_{OA} > 0$ depending on the system's bandwidth. BA and AQ_1 should be tangent to each other at A, yields:

$$\frac{dy_A}{dx_A} = -\left((2a_{Ub}(x_A - x_P))^{\frac{1}{2}}\right)'$$
$$= -\frac{a_{Ub}}{\sqrt{2a_{Ub}(x_A - x_P)}} = -k_{OA} \tag{24}$$

Values of x_A, y_A, x_P can be solved using (22), (23) and (24). With the minimum velocity defined as v_{Lb}, x_B can be

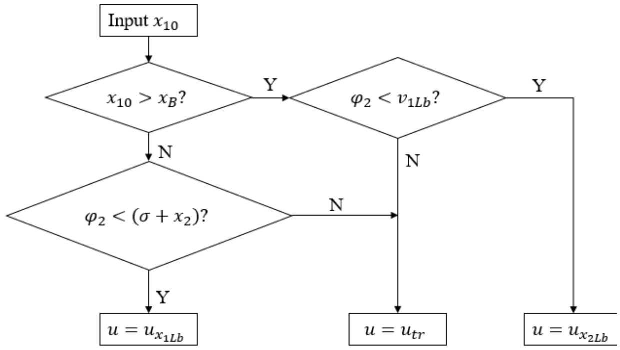

FIGURE 4. Variable structure law for the double integer.

solved as

$$x_B = \frac{y_B^2}{2a_{Ub}} + x_P \tag{25}$$

Thus the sub-time optimal sliding surface can be derived as

$$\sigma(x_1, x_2) = \begin{cases} -k_{OA}(x_1 - x_{1Lb}) - x_2, & x_1 \le x_A \\ -\sqrt{2a_{Ub}(x_1 - x_P)} - x_2, & x_A < x_1 < x_B \end{cases} \tag{26}$$

To apply the variable structure law, three controllers of the system can be derived as

Position lower bounded controller:

$$u_{x_{1Lb}} = \begin{cases} -k_{OA}x_2 + k_1\sigma, & x_1 \le x_A \\ -\dfrac{a_{Ub}x_2}{\sqrt{2a_{Ub}(x_1 - x_P)}} + k_2\sigma, & x_A < x_1 < x_B \end{cases} \tag{27}$$

Velocity lower bounded controller:

$$u_{x_{2Lb}} = -k_3(x_2 - v_{Lb}) \tag{28}$$

Tracking controller

$$u_{tr} = \dot{\varphi}_2 - \bar{x}_1 - k_5\bar{x}_2 \tag{29}$$

where φ_2 is the virtual controller for x_2

$$\varphi_2 = -k_4\bar{x}_1 + \dot{x}_d \tag{30}$$

x_d is the target trajectory, $\bar{x}_1 = (x_1 - x_d)$, $\bar{x}_2 = (x_2 - \varphi_2)$, $k_i > 0, i = 1, 2, \ldots 5$ Variable structure law is defined as in Fig.4 and the following three important properties hold under this VS law:

i. Practical phase trajectory is always beyond Γ_2 in terms of x_2
ii. x_1 will stay at x_{1Lb} as long as x_d is smaller than x_{1Lb}
iii. Tracking tends to be fulfilled once x_d is bigger than x_{1Lb}

Note that φ_2 is a virtual controller for x_2 aims at tracking the target trajectory lower bounded by Γ_2 which means that when states under tracking control attempts to go smaller then Γ_2, they will be constrained to slides on Γ_2, thus i holds. When target trajectory is on the line C_4Q_3, without no loss of generality suppose the target state is at Q_2, though u_{tr} may be enabled by VS law, tracking response Γ_3 from lower bound x_{1Lb} must intersects with Γ_2 which will bring states

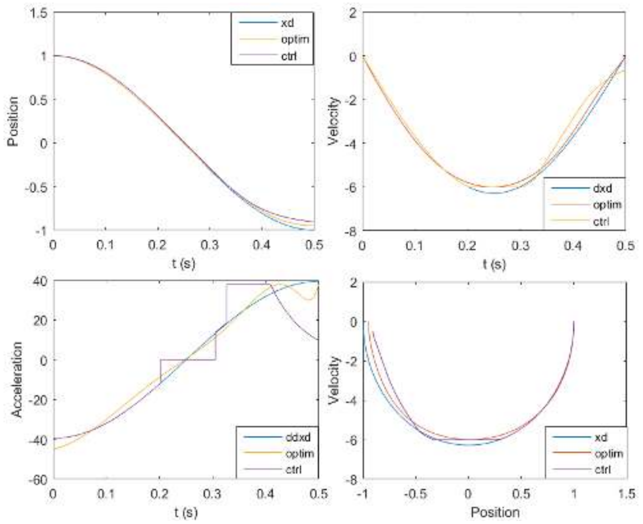

FIGURE 5. States under controller A and B in phase plane.

back to the lower bound thus ii holds. After $x_d > x_{1Lb}$, no intersections with Γ_2 appears under u_{tr}, tracking tends to be fulfilled which implies iii.

With some more insight into this process, especially during the transient process, overshoot may be caused by large transient gain, boundary layer of sliding mode control and sampling noise. Experimental results in section 5 shows that such overshoot is acceptable, whereas improved performance of transient response can be particularly designed as in [37] by the methods aforementioned in Introduction. And as to the possibly abrupt jump of control signal when switches take place, an adaptive sliding slope [23] is recommended.

C. SIMULATION AND DISCUSSION

Simulation results of controller A and B are given in Fig. 5 for the double integer. Tag *xd* refers to the target trajectory; *optim* refers to the results of controller A and *ctrl* refers to controller B. It can be seen that when the trajectory is feasible, tracking can be fulfilled and constraints on velocity and position are satisfied when target trajectory is infeasible.

Since the target trajectory is given by a standard *sin* function, the ideal constrained trajectory can be calculated accurately. Tracking errors to this ideal constrained trajectory by controller A and B are given in Fig 6. To improve the performance of controller A, a more proper trajectory generation method should be used so that the constrained optimized trajectory can fit better into the ideal trajectory. Meanwhile, controller A needs a heave prediction time sufficiently lone that may need to reach 1/2 average period of heave motion to reliably bound the compensation process, this is also not an easy task with the only use of an MRU. Controller B, on the other hand, only need to adjust its approaching gain k_{OA} to get a better performance and thus is more suitable to be applied to AHCs. The following experiments are based on this VS controller.

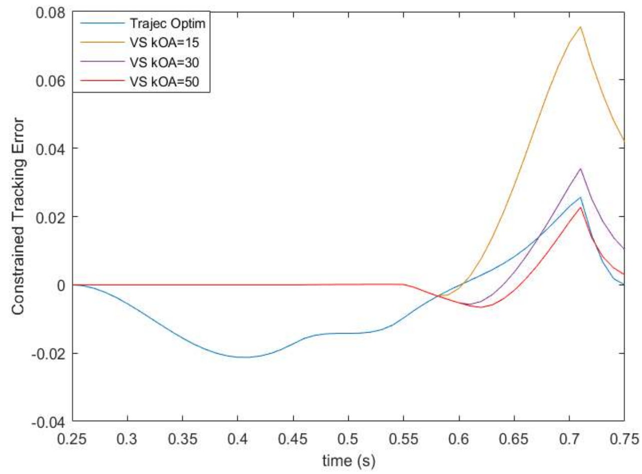

FIGURE 6. Tracking errors to ideal constrained trajectory.

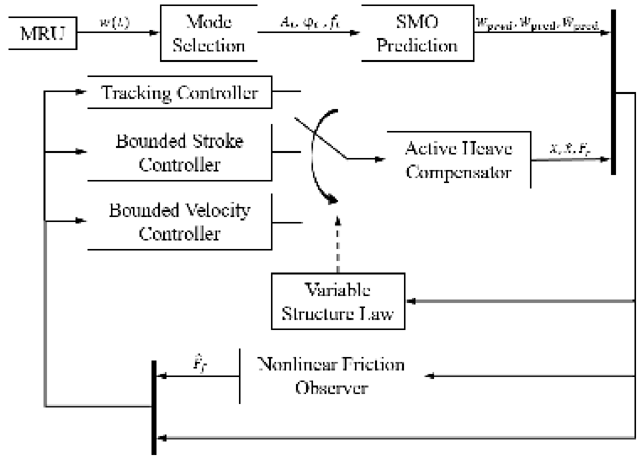

FIGURE 7. Controller scheme for AHC.

IV. CONTROLLER DERIVATION

Schematic of the controllers for AHC is shown in Fig 7. Measured heave by MRU is the input of the total system and the time delay of MRU is compensated by heave prediction algorithm introduced in section 2. The predicted heave motion is the input to the control system, together with the system's other variables including position, velocity and tension of the rope. With the friction observed by the modified nonlinear friction observer, there are mainly three controllers need to be derived: tracking controller, boundary stroke controllers and boundary velocity controllers. These controllers are derived using back-stepping method as follows.

Dynamic model of the system is as follows

$$\begin{aligned}
\dot{x}_1 &= x_2 \\
\dot{x}_2 &= \frac{1}{m_{eq}}(f_2 - \hat{F}_f - \delta F_f + A_1 \bar{x}_3) \\
\dot{\bar{x}}_3 &= f_4 u - f_3 - f_5
\end{aligned}$$

The aim of the tracking controller is to make the system's output $y_1 = x_1$ track the predicted heave motion $\frac{1}{2} w_{pred}$.

Define the tracking error as $\bar{x}_1 = x_1 - \frac{1}{2}w_{pred}$. Define a Lyapunov function for $\bar{x}_1$ as

$$V_1 = \frac{1}{2}\bar{x}_1^2 \tag{31}$$

To make $\bar{x}_1 = 0$ the asymptotically stable point, a virtual control of x_2 can be chosen as

$$\varphi_2 = \frac{1}{2}\dot{w}_{pred} - k_1\bar{x}_1 \tag{32}$$

With the tracking error for x_2 defined as $\alpha_2 = x_2 - \varphi_2$, derivative of V_1 is written as

$$\dot{V}_1 = \bar{x}_1\left(\alpha_2 + \varphi_2 - \frac{1}{2}w_{pred}\right) \leq -k_1\bar{x}_1^2 + \bar{x}_1\alpha_2 \tag{33}$$

To make α_2 converges to 0 asymptotically, define

$$V_2 = V_1 + \frac{1}{2}\alpha_2^2 \tag{34}$$

We have the derivative of V_2 calculated as

$$\dot{V}_2 \leq \dot{V}_1 + \alpha_2\left(\frac{1}{m_{eq}}\left(f_2 - \hat{F}_f - \delta F_f + A_1\bar{x}_3\right) - \dot{\varphi}_2\right) \tag{35}$$

The virtual controller for x_3 is chose to be

$$\varphi_3 = \frac{1}{A_1}\left(\hat{F}_f - f_2 - m_{eq}\bar{x}_1 + m_{eq}\left(\dot{\varphi}_2 + v\right)\right) \tag{36}$$

where $v = -\rho sign(\alpha_2)$ with $\rho \geq |\frac{\delta F_f}{m_{eq}}|$, then we have

$$\dot{V}_2 \leq -k_1\bar{x}_1^2 + \left(-\rho + \left|-\frac{\delta F_f}{m_{eq}}\right|\right)|\alpha_2| + \frac{A_1\alpha_2}{m_{eq}}\alpha_3 \tag{37}$$

where $\alpha_3 = \bar{x}_3 - \varphi_3$

Define

$$\begin{aligned} V_3 &= V_2 + \frac{1}{2}\alpha_3^2 \\ \dot{V}_3 &\leq \dot{V}_2 + \alpha_3\left(\left(f_4 u - f_3 - f_5\right) - \dot{\varphi}_3\right) \end{aligned} \tag{38}$$

To make the derivative of V_3 negative semidefinite, a tracking controller u_{tr} can be chosen as

$$u_{tr} = \frac{1}{f_4}\left(f_3 + f_5 + \dot{\varphi}_3 - \frac{A_1\alpha_2}{m_{eq}} - k_2\alpha_3\right) \tag{39}$$

then

$$\dot{V}_3 \leq -k_1\bar{x}_1^2 + \left(-\rho + \left|-\frac{\delta F_f}{m_{eq}}\right|\right)|\alpha_2| - k_2\alpha_3^2 \leq 0 \tag{40}$$

Since no trajectory can stay identically at points where $\dot{V}_3 = 0$ except at the origin, so the origin is asymptotically stable which implies that tracking can be fulfilled.

Note that to tune the aforementioned tracking controller, there are 3 parameters needed to be adjusted which are k_1, k_2, ρ, while k, μ of the friction observer are decoupled from the controller which means that tuning process of the control system is easier than the DOBNC or EDOBNC while the tracking performance are much the same when trajectory is within the feasible area.

When turns to the position upper boundary or lower boundary controller, a sub time optimal sliding surface regulating process should be designed first as introduced in section 3, then with the new definition to position error and virtual control of x_2 as

$$\begin{aligned} \bar{x}_{1u} &= x_1 - x_{1Ub} \\ \varphi_{21u} &= \sigma_{1u}\left(x_1, x_2\right) + x_2 \end{aligned} \tag{41}$$

The position upper boundary controller can be derived as

$$u_{1u} = \frac{1}{f_4}\left(f_3 + f_5 + \dot{\varphi}_{31u} - \frac{A_1\alpha_{21u}}{m_{eq}} - k_{21u}\alpha_{31u}\right) \tag{42}$$

And similarly, the position lower boundary control is

$$u_{1L} = \frac{1}{f_4}\left(f_3 + f_5 + \dot{\varphi}_{31L} - \frac{A_1\alpha_{21L}}{m_{eq}} - k_{21L}\alpha_{31L}\right) \tag{43}$$

Besides position boundary controllers, velocity boundary controllers are also necessary. These two controllers can be derived using the aforementioned back-stepping method with an exchange of virtual controller φ_2 into $\varphi_{2u} = v_{Ub}$ or $\varphi_{2L} = v_{Lb}$, then bounded velocity controllers can be derived as

$$u_{2u} = \frac{1}{f_4}\left(f_3 + f_5 + \dot{\varphi}_{3u} - \frac{A_1\alpha_{2u}}{m_{eq}} - k_{2u}\alpha_{3\mathrm{u}}\right) \tag{44}$$

$$u_{2L} = \frac{1}{f_4}\left(f_3 + f_5 + \dot{\varphi}_{3L} - \frac{A_1\alpha_{2L}}{m_{eq}} - k_{2L}\alpha_{3L}\right) \tag{45}$$

Variable structure law is derived as, when the virtual control φ_2 exceeds the boundaries defined by the constraints, then corresponding boundary controller is enable, otherwise tracking controller is enable. Feasible area of the active heave compensation system in this paper is shown in fig. 8 with the boundary:

$$\begin{aligned} -0.12 &\leq x_1 \leq 0.12 \\ -0.09 &\leq x_2 \leq 0.09 \\ -0.1 &\leq \dot{x}_2 \leq 0.1 \end{aligned}$$

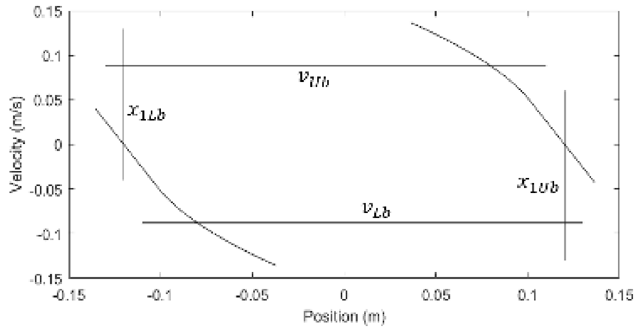

FIGURE 8. Constraints in phase plane.

V. EXPERIMENTAL RESULTS

The proposed controller is verified on an experimental equipment as shown in Fig.9. A storage winch driven by servo valve is adopted to simulate the vessel's heave motion and a payload with the mass of 4T is suspended by a 25mm diameter cable. Related position, velocity, acceleration signal and

FIGURE 9. Experimental equipment.

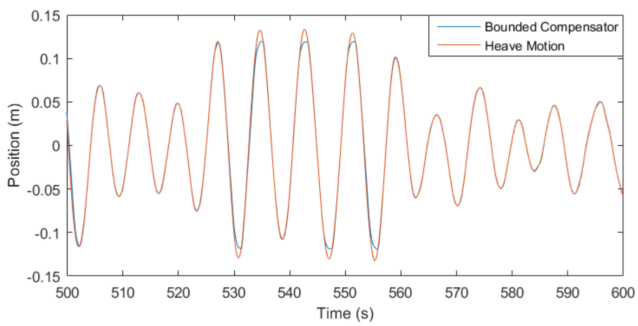

FIGURE 10. Input and the compensated heave motion.

cable tension, pressures of the hydraulic system are measured by certain sensors, respectively.

Angular acceleration of the winch is treated as the MRU measured acceleration in practical use and time delay is set to 0.5s according to the MRU used in this sea trial. Upper and lower heave compensation bounds are set to be −0.24m and 0.24m. Velocity bounds are set to be −0.18m/s and 0.18m/s. Fig.10 shows the input heave motion and AHCS compensated heave motion. When heave motion is within the compensation range, heave of payload is within 0.01m. This result is almost the same as the one controlled by EDOBNC proposed in [10]. Boundedness of this process can be better illustrated by Fig.11 in phase plane spanned by piston's positon and velocity (which are multiplied by 2 for the consistency with that of the payload). Obviously displacement never exceeds the boundary.

Observed friction is shown in Fig.12. Though accurate measurement of friction is almost impossible, its estimates by the modified nonlinear observer displays similar practical regularities as in [38]–[40] which are, the dynamic behavior of friction when velocity is varied during unidirectional motion, and hysteresis in the relation between friction and

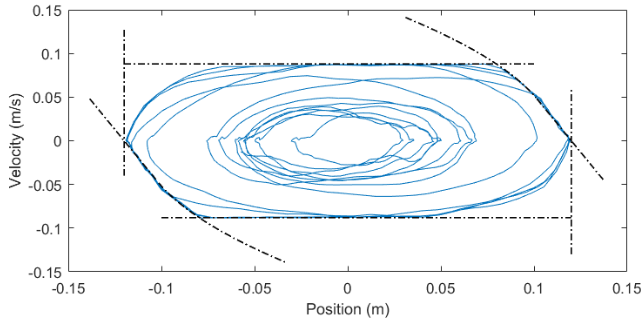

FIGURE 11. Constraints and tracking trajectories in phase plane.

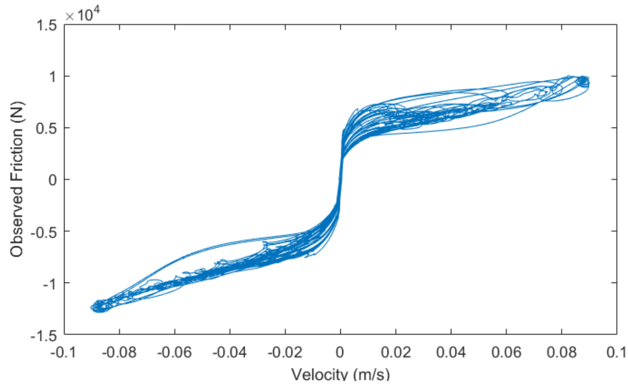

FIGURE 12. Friction and velocity relation of the friction observer.

velocity. It should be noted that there is indeed residual between practical and estimated friction, but attempt to compensate for the effects of friction, without resorting to high robust gain is successfully fulfilled by this modified observer during parameter tuning process of these experiments and the reduction on the number of control tuning is obvious.

VI. CONCLUSION

In this paper, a robustly state constrained variable structure controller is proposed for active heave compensation systems to handle the situation when vessel's heave motion exceeds the predesigned compensation range or velocity range. Effectiveness of the controller is verified by experiment. A modified nonlinear friction observer is proposed to compensate for the effects of friction without resorting to high robust gain.

It should be noted that although the algorithm is derived from an AHC, other compensation systems with similar constraints can also be used, moreover, controller design for other hydraulic equipment such as hydraulic cranes with similar constraints can also refer to the method in this paper. Yet payload of these experiments is in the air, further experiments such as payload in the water are still recommended.

REFERENCES

[1] T. Z. Liu *et al.*, "Performance evaluation of active wireline heave compensation systems in marine well logging environments," *Geo-Marine Lett.*, vol. 33, no. 1, pp. 83–93, Feb. 2013.

[2] L. J. Li and S. J. Liu, "Modeling and simulation of active-controlled heave compensation system of deep-sea mining based on dynamic vibration absorber," in *Proc. IEEE Int. Conf. Mechatron. Autom.*, Aug. 2009, pp. 1337–1341.

[3] J. P. Blanchet and T. J. Reynolds, "Crane hook heave compensator and method of transferring loads," U.S. Patent 4 003 472, Jan. 10, 1977.
[4] R. M. Alkan, "Reduction of heave, pitch and roll effects in hydrographic surveying," *Surv. Rev.*, vol. 37, no. 289, pp. 208–217, Jul. 2013.
[5] J. K. Woodacre, R. J. Bauer, and R. A. Irani, "A review of vertical motion heave compensation systems," *Ocean Eng.*, vol. 104, pp. 140–154, Aug. 2015.
[6] A. Huster, H. Bergstrom, J. Gosior, and D. White, "Design and operational performance of a standalone passive heave compensation system for a work class ROV," in *Proc. OCEANS Conf.*, Oct. 2009, pp. 2287–2294.
[7] M. J. Ormond, "Depth compensated subsea passive heave compensator," U.S. Patent 7 934 561 B2, Mar. 5, 2011.
[8] J. Ni, S. J. Liu, M. F. Wang, X. Z. Hu, and Y. Dai, "The simulation research on passive heave compensation system for deep sea mining," in *Proc. IEEE Int. Conf. Mechatron. Autom.*, Aug. 2009, pp. 5111–5116.
[9] F. R. Driscoll, M. Nahon, and R. G. Lueck, "A comparison between ship-mounted and cage-mounted passive heave compensation systems," in *Proc. Oceans Conf.*, Oct. 1998, pp. 1449–1454.
[10] S. Z. Li, J. H. Wei, K. Guo, and W. L. Zhu, "Nonlinear robust prediction control of hybrid active-passive heave compensator with extended disturbance observer," *IEEE Trans. Ind. Electron.*, vol. 64, no. 8, pp. 6684–6694, Aug. 2017.
[11] N. Woodall-Mason and J. R. Tilbe, "Value of heave compensators to floating drilling," *J. Petroleum Technol.*, vol. 28, no. 8, pp. 938–946, Aug. 1976.
[12] A. Bemporad, F. Borrelli, and M. Moraro, "Model predictive control based on linear programming the explicit solution," *IEEE Trans. Autom. Control*, vol. 47, no. 12, pp. 1974–1985, Dec. 2002.
[13] D. Q. Mayne, J. B. Rawlings, C. V. Rao, and P. O. M. Scokaert, "Constrained model predictive control: Stability and optimality," *Automatica*, vol. 36, no. 6, pp. 789–814, 2000.
[14] A. Bemporad, "Reference governor for constrained nonlinear systems," *IEEE Trans. Autom. Control*, vol. 43, no. 3, pp. 415–419, Mar. 1998.
[15] J. Wolff and M. Buss, "Invariance control design for constrained nonlinear systems," *IFAC Proc. Vol.*, vol. 38, no. 1, pp. 37–42, 2005.
[16] J. Wolff, C. Weber, and M. Buss, "Continuous control mode transitions for invariance control of constrained nonlinear systems," in *Proc. 46TH IEEE Conf. Decis. control*, Dec. 2007, pp. 5571–5576.
[17] H. Richter, B. D. O'Dell, and E. A. Misawa, "Robust positively invariant cylinders in constrained variable structure control," *IEEE Trans. Autom. Control*, vol. 52, no. 11, pp. 2058–2069, Nov. 2007.
[18] K. P. Tee, S. S. Ge, and E. H. Tay, "Barrier Lyapunov functions for the control of output-constrained nonlinear systems," *Automatica*, vol. 45, no. 4, pp. 918–927, Apr. 2009.
[19] K. P. Tee and S. S. Ge, "Control of nonlinear systems with full state constraint using a barrier lyapunov Function," in *Proc. 48TH IEEE Conf. Decis. Control*, Dec. 2009, pp. 8618–8623.
[20] P. Mhaskara, N. H. El-Farrab, and P. D. Christofides, "Stabilization of nonlinear systems with state and control constraints using Lyapunov-based predictive control," *Syst. Control Lett.*, vol. 55, no. 8, pp. 650–659, 2006.
[21] K. B. Ngo, R. Mahony, and J. Zhong-Ping, "Integrator backstepping using barrier functions for systems with multiple state constraints," in *Proc. 44TH IEEE Conf. Decis. Control Eur. Control*, Dec. 2005, pp. 8306–8312.
[22] J. H. Fang, F. Guo, Z. Chen, and J. H. Wei, "Improved sliding-mode control for servo-solenoid valve with novel switching surface under acceleration and jerk constraints," *Mechatronics*, vol. 43, pp. 66–75, May 2017.
[23] L. Y. Pao and G. F. Franklin, "Proximate time-optimal control of third-order servomechanisms," *IEEE Trans. Autom. Control*, vol. 38, no. 4, pp. 560–580, Apr. 1993.
[24] J. Neupert, T. Mahl, B. Haessig, O. Sawodny, and K. Schneider, "A heave compensation approach for offshore cranes," in *Proc. Amer. Control Conf.*, Jun. 2008, pp. 538–543.
[25] H. Yu, J. H. Wei, J. H. Fang, G. Sun, and H. J. Zhang, "Predictive robust control based on higher-order sliding mode for passive heave compensator with hydraulic transformer," in *Proc. BATH/ASME Symp. Fluid Power Motion Control*, 2018, pp. V001T01A017–V001T01A017.
[26] J. Yao, Z. Jiao, D. Ma, and L. Yan, "High-accuracy tracking control of hydraulic rotary actuators with modeling uncertainties," *IEEE/ASME Trans. Mechatron.*, vol. 19, no. 2, pp. 633–641, Apr. 2014.
[27] B. Yao, F. Bu, J. Reedy, and G. T.-C. Chiu, "Adaptive robust motion control of single-rod hydraulic actuators: Theory and experiments," *IEEE/ASME Trans. Mechatron.*, vol. 5, no. 1, pp. 79–91, Mar. 2000.
[28] J. Yao, Z. Jiao, and D. Ma, "A practical nonlinear adaptive control of hydraulic servomechanisms with periodic-like disturbances," *IEEE/ASME Trans. Mechatronics*, vol. 20, no. 6, pp. 2752–2760, Dec. 2015.
[29] C. Kaddissi, J. P. Kenne, and M. Saad, "Identification and real-time control of an electrohydraulic servo system based on nonlinear backstepping," *IEEE/ASME Trans. Mechatronics*, vol. 12, no. 1, pp. 12–22, Feb. 2007.
[30] J. Yao, Z. Jiao, and D. Ma, "Extended-state-observer-based output feedback nonlinear robust control of hydraulic systems with backstepping," *IEEE Trans. Ind. Electron.*, vol. 61, no. 11, pp. 6285–6293, Nov. 2014.
[31] B. Friedland and Y.-J. Park, "On adaptive friction compensation," *IEEE Trans. Autom. Control*, vol. 37, no. 10, pp. 1609–1612, Oct. 1992.
[32] T. I. Fossen, *Guidance and Control of Ocean Vehicles*. Hoboken, NJ, USA: Wiley, 1994.
[33] A. R. J. M. Lloyd, *Seakeeping Ship Behaviour in Rough Weather*. New York, NY, USA: Ellis Horwood, 1998.
[34] V. I. Utkin, *Sliding Modes in Control and Optimization*. New York, NY, USA: Springer, 2013.
[35] J. Yao, W. Deng, and Z. Jiao, "Adaptive control of hydraulic actuators with LuGre model-based friction compensation," *IEEE Trans. Ind. Electron.*, vol. 62, no. 10, pp. 6469–6477, Oct. 2015.
[36] J. B. Gamble and N. D. Vaughan, "Comparison of sliding mode control with state feedback and PID control applied to a proportional solenoid valve," *J. Dyn. Syst., Meas., Control*, vol. 118, pp. 434–438, Sep. 1996.
[37] X. L. Wang, Y. A. Zhang, and H. L. Wu, "Sliding mode control based impact angle control guidance considering the seeker?s field-of-view constraint," *ISA Trans.*, vol. 61, pp. 49–59, Mar. 2016.
[38] D. P. Hess and A. Soom, "Friction at a lubricated line contact operating at oscillating sliding velocities," *J. Tribol.*, vol. 112, no. 1, pp. 147–152, Jan. 1990.
[39] C. Canudas de Wit, H. Olsson, K. J. Astrom, and P. Lischinsky, "A new model for control of systems with friction," *IEEE Trans. Autom. Control*, vol. 40, no. 3, pp. 419–425, Mar. 1995.
[40] O. Heipl and H. Murrenhoff, "Friction of hydraulic rod seals at high velocities," *Tribol. Int.*, vol. 85, pp. 66–73, May 2015.

HUAN YU received the bachelor's degree in mechatronic engineering from Zhejiang University, Hangzhou, China, in 2014, where he is currently pursuing the Ph.D. degree in mechatronic engineering. His research interests include robust control, optimal control, and fluid power transmission.

YING CHEN received the master's degree in fluid power transmission and control from Zhejiang University, Hangzhou, China, in 2013. She is currently an Assistant Engineer of the Hangzhou Applied Acoustics Research Institute. Her research interests include design and analysis of hydraulic system, hydraulic fault diagnosis technology, and hydraulic integrated support technology.

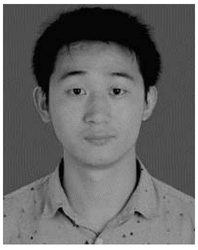

WENZHUO SHI received the bachelor's degree in mechatronic engineering from Zhejiang University, Zhejiang, China, where he is currently pursuing the Ph.D. degree in mechatronic engineering. His research interests include hydraulic components, nonlinear control of electro-hydraulic systems and industrial automation.

YI XIONG received the Ph.D. degree in fluid power transmission and control from Zhejiang University, Hangzhou, China, in 2015. He is currently an Engineer of the Nantong Metalforming Equipment Co., LTD., Nantong, China. His current research interests include the hydraulic presses, advanced motion control of electro-hydraulic systems, synchronization control, and industry automation.

JIANHUA WEI received the Ph.D. degree in fluid power transmission and control from Zhejiang University, Hangzhou, China, in 1995, where he is currently a Professor of the State Key Laboratory of Fluid Power and Mechatronic Systems. His current research interests include actuators, fluid power, and transmission.